IEEE Access
Multidisciplinary ⋮ Rapid Review ⋮ Open Access Journal

Received 22 May 2022, accepted 9 July 2022, date of publication 13 July 2022, date of current version 18 July 2022.

*Digital Object Identifier 10.1109/ACCESS.2022.3190687*

RESEARCH ARTICLE

# A Small Metaline Array Antenna for Circularly Polarized Dual-Band Beam-Steering

**HISAMATSU NAKANO, (Life Fellow, IEEE), TOMOKI ABE, (Member, IEEE), AND JUNJI YAMAUCHI, (Life Fellow, IEEE)**

Science and Engineering Department, Hosei University, Tokyo 184-8584, Japan

Corresponding author: Hisamatsu Nakano (hymat@hosei.ac.jp)

This work was supported in part by the Japan Society for the Promotion Science (JSPS) KAKENHI under Grant JP21K04068.

**ABSTRACT** A circularly polarized (CP), small, beam-steerable antenna is realized using bent metalines. The antenna has the following features: 1) dual-band operation at low frequency $f_{LOW}$ (wavelength $\lambda_{LOW}$) and at high frequency $f_{HIGH}$ (wavelength $\lambda_{HIGH}$); 2) a small antenna volume of less than $0.01\lambda_{LOW}^3$; 3) a small antenna height on the order of $\lambda_{LOW}/100$; 4) a small conducting antenna footprint of $0.62\lambda_{LOW} \times 0.49\lambda_{LOW}$; and 5) a phased array antenna consisting of minimum array elements (two elements). Firstly, the antenna characteristics of straight and bent metalines are briefly summarized. Secondly, it is shown that an array antenna composed of two bent metalines forms a CP broadside beam at $f_{LOW}$ using an equal-amplitude/in-phase excitation mode. This is also shown to be true at $f_{HIGH}$. Thirdly, each of the obtained CP broadside beams at $f_{LOW}$ and $f_{HIGH}$ is steered within the H-plane. The array antenna is found to have a CP beam that is steerable across a region of $\theta = -40°$ to $\theta = +30°$ at $f_{LOW}$ and $\theta = -40°$ to $\theta = +25°$ at $f_{HIGH}$, with an axial ratio of less than 3 dB. During the beam steering, the gain deviation from its maximum value is found to be small: 1.7 dB at $f_{LOW}$ and 1.4 dB at $f_{HIGH}$.

**INDEX TERMS** Beam steering, circular polarization, dual band operation, metaline.

## I. INTRODUCTION

Helical antennas [1]–[3], spiral antennas [4]–[6], curl antennas [7]–[9], and loop antennas [10], [11] are representative circularly polarized (CP) antennas that radiate their beams in the broadside direction. Communication systems using CP antennas do not need polarization alignment between the transmitting and receiving antennas. However, it is required that the broadside CP radiation beam from the transmitting antenna faces in the direction of the receiving antenna to increase communication efficiency. This is realized by mechanically/physically or electrically tilting the transmitting antenna such that the beam is directed toward the receiving antenna. Electrical tilting has an advantage over mechanical tilting in that the antenna position remains unchanged. So far, CP tilted beam formation has been discussed for various CP antennas, as shown in Table 2 of the Appendix.

The associate editor coordinating the review of this manuscript and approving it for publication was Mohammad Zia Ur Rahman.

The CP helical antenna has a long structure composed of a single arm of more than 7 turns above the ground plane (GNP) [1]. Detailed analysis of the current distribution along the long helical arm has led to the creation of a CP short helical antenna whose arm is composed of only approximately two turns (hence, the antenna height is small: on the order of 1/5 wavelength [12]). The short helical antenna has been used as an array antenna element. It is found that an array using this helical element can form a tilted CP beam by mechanically rotating the helical elements around their axes [13].

The CP wave from the two-arm spiral antenna in [4] travels in the two directions normal to the spiral-arm plane when the spiral arms are excited in the odd mode (equal-amplitude/180°-phase difference excitation mode). This bidirectional CP beam can be changed into a unidirectional CP beam by backing the spiral arms with a conducting plate (reflector plate). The antenna height above the reflector plate in this case is chosen to be approximately l/4 wavelength at the design frequency. It is worth mentioning that the CP single-arm spiral antenna in [14], [15] is a modification of

the two-arm spiral antenna and generates a tilted beam in a certain direction. The antenna height above the reflector plate in [14] is 1/4 wavelength.

The curl antenna in [7] is an antenna derived from the CP single-arm spiral antenna, where the number of arm-winding turns is drastically reduced to be small, typically, less than two. The height of the curled arm above the GNP is approximately 1/7 wavelength. It has been reported that a tilted beam from an array antenna composed of the curl elements can be realized by mechanically rotating the arrayed curl elements around their axes, as with the short helical elements in [13].

The loop antennas in [16], [17] radiate a linearly polarized (LP) wave. In contrast, the loop antenna system in [18], where a perturbation element [19] is added to each of two concentrically arrayed loops, acts as a CP antenna. It has been found that a CP tilted beam can be realized by electrically changing the phases of the two loops, where the inner loop has a one-wavelength circumference and the outer loop has a two-wavelength circumference, both being located l/16 wavelength above the reflector plate at the design frequency [18].

We recall that the abovementioned CP antenna arrays, except for the CP loop array [18], have their beams tilted in a certain *fixed* direction within the elevation plane; the direction of the CP beam is *mechanically/physically* adjusted, not electrically adjusted. Also, we recall that these tilted CP beams are designed for single frequency band operation. With the advancement of modern communication systems, antennas whose CP beam direction is *electrically* controlled have been receiving attention as beam-steerable antennas [20]–[26]. In addition, modern communication systems have been accelerating development of dual-frequency CP operation antennas from the viewpoint of increasing communication capability [20].

In this context, this paper presents a novel, *electrically* steerable, small CP beam antenna with dual-band operation.

The antenna has the following novelties/features: (1) beam-steerable operation around a low frequency of $f_{\mathrm{LOW}}$ (wavelength $\lambda_{\mathrm{LOW}}$) and a high frequency of $f_{\mathrm{HIGH}}$ (wavelength $\lambda_{\mathrm{HIGH}}$); (2) a small volume of less than $0.01\lambda_{\mathrm{LOW}}^3$; (3) a small antenna height on the order of $\lambda_{\mathrm{LOW}}/100$; (4) a conducting small antenna footprint (parallel to the ground plane) of $0.62\lambda_{\mathrm{LOW}} \times 0.49\lambda_{\mathrm{LOW}}$; and (5) a phased array antenna consisting of minimum array elements (two elements).

Note that feature (3) contributes to reducing the protrusion of the antenna when it is mounted on a surface, such as a wall, ceiling, drone, helicopter, or cubic satellite. Feature (4) makes installation of the antenna in a limited space more feasible. To the best of the authors' knowledge, there are no antennas available that have simultaneously features (1)-(5). For comparison, previous antennas with a CP tilted beam are presented in the Appendix (see Table 2).

A potential application of the presented antenna is illustrated in Fig. 1, where the antenna enables multi-communications toward different targets, performing CP beam-steering at two separate frequencies. This is superior

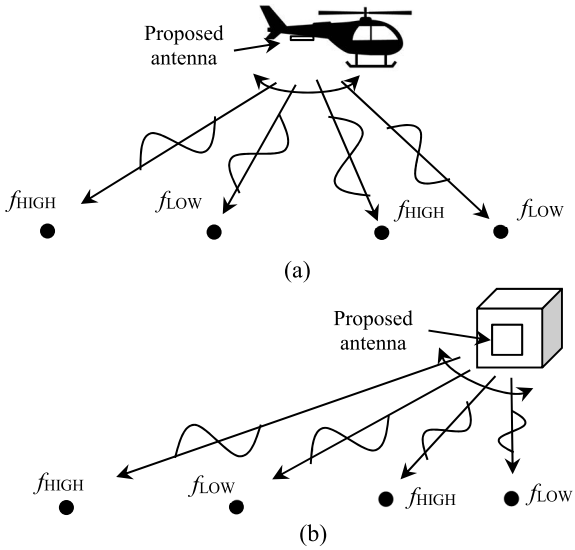


**FIGURE 1. Application examples of the present antenna using two frequencies. (a) Antenna mounted on a helicopter. (b) Antenna mounted on a cubic satellite.**

to the ability of conventional slot, microstrip line, and SIW antennas.

This paper is composed of five sections. Section II briefly summarizes a straight metaline composed of P-type metaatoms. It is described that a CP broadside beam is only obtained around a single specific frequency (transition frequency $f_{\mathrm{T}}$). Subsequently, the straight metaline is bent so that CP broadside beams are obtained at two design frequencies, $f_{\mathrm{LOW}}$ and $f_{\mathrm{HIGH}}$ outside $f_{\mathrm{T}}$. Section III presents a novel small array antenna composed of two bent metalines. The CP characteristics when the two bent metalines are excited in equal-amplitude/in-phase mode are revealed. In Section IV, beam steering for an array antenna of two bent metalines with equal-amplitude/different-phase mode excitation is simulated. The simulation results are confirmed by measuring a fabricated array antenna. The angle range is clarified for the steered beam at $f_{\mathrm{LOW}}$ and $f_{\mathrm{HIGH}}$. Section V summarizes the obtained results. The simulation in this paper is performed using an electromagnetic solver based on the finite integral method [27].

As seen from the above paragraph, the contents of this paper are regarding the realization of a small beam-steering antenna and obviously differ from those of the recent paper (*i.e.*, formation of a fixed fan-beam) [28], although a metaline is used as an array element.

For better understanding of the advantage of the presented antenna, it is worth comparing a reconfigurable antenna technique [29]–[31] with a phased array antenna technique [32]. In a reconfigurable antenna, the beam is controlled by switching circuits and hence the beam direction cannot be continuously/seamlessly controlled. On the other hand, in a phased array antenna (such as the presented antenna in this paper), the beam is seamlessly steered by controlling the excitation phase difference between the two elements.

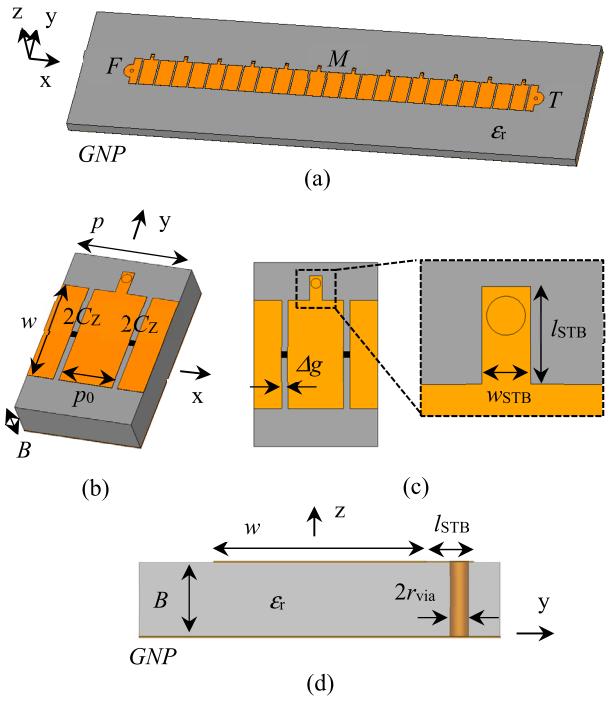


**FIGURE 2.** Straight metaline composed of P-type metaatoms. (a) Perspective view of the metaline. (b) Perspective view of the metaatom. (c) Top view of the metaatom. (d) Side view of the metaatom.

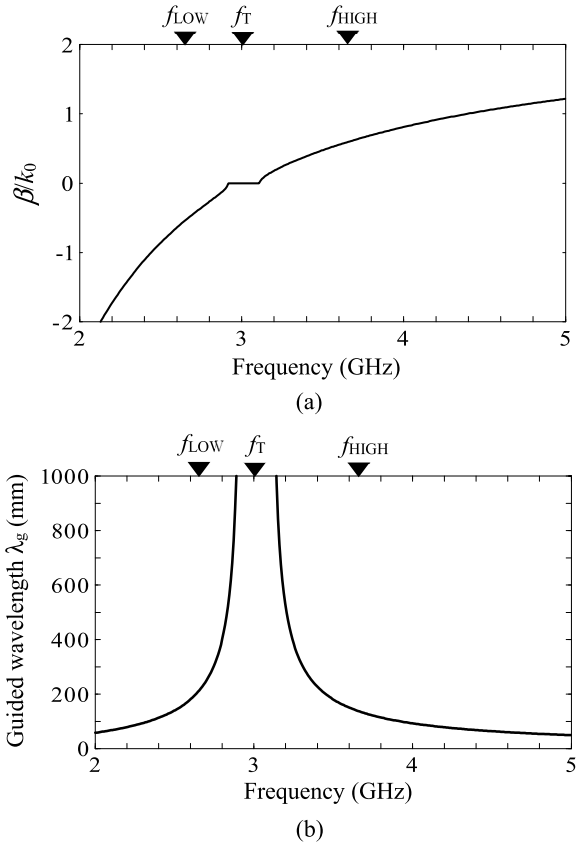


**FIGURE 3.** Dispersion diagram for the P-type metaatom. (a) Normalized propagation phase constant $\beta/k_0$, where $\beta$ is the propagation phase constant for the current on the metaatom and $k_0$ is the wave number in free space. (b) Guided wavelength $\lambda_g$, where $f_{LOW}$ and $f_{HIGH}$ are used as design frequencies.

In addition, it should be emphasized that the presented phased array antenna can steer the radiation beam by fixing the operation frequency at *two* frequencies of $f_{LOW}$ and $f_{HIGH}$. This frequency-independent beam steering cannot be obtained by leaky-wave antennas, where the beam is steered with change in the frequency [33].

## II. A STRAIGHT METALINE AND A BENT METALINE

### A. STRAIGHT METALINE

Fig. 2 shows a modified microstrip line, which is composed of repeating subwavelength strip segments. These strip segments are printed on a dielectric substrate of relative permittivity $\varepsilon_r$ and thickness $B$. The width of the line is $w$. This straight line, which is an extended version of the composite right/left handed transmission line [34], is designated as the straight P-type metaline (or simply, the straight metaline) throughout this paper [35].

A region of length $p$ is defined as the P-type metaatom: $p = 2(p_0 + \Delta g)$, where $p_0$ is the strip length and $\Delta g$ is the gap between neighboring strips, into which a chip capacitor of capacitance $2C_Z$ is inserted. The central strip of length $p_0$ and width $w$ for the metaatom includes a stub of length $l_{STB}$ and width $w_{STB}$. Point $F$ is the feed point, which is connected to the center conductor of a coaxial line. The outer conductor of the coaxial line is connected to the ground plane, GNP. Point $T$ is located at the arm end and connected to the GNP through resistive load $R_B$ (= 50 ohms). Note that the stub located on the left side of line $FT$ is short-circuited to the GNP.

**TABLE 1.** Parameters for the P-type metaatom.

| Symbol | Value | Symbol | Value |
|---|---|---|---|
| $B$ | 3.2 mm | $\varepsilon_r$ | 2.6 |
| $p$ | 10.0 mm | $w$ | 8.8 mm |
| $p_0$ | 4.5 mm | $g$ | 0.5 mm |
| $w_{STB}$ | 1.0 mm | $l_{STB}$ | 2.0 mm |
| $2r_{via}$ | 0.8 mm | $2C_Z$ | 1.3 pF |

The dispersion diagram for the P-type metaatom is shown in Fig. 3, where $\beta$ denotes the propagation phase constant for the current flowing along the metaatom, and $k_0$ denotes the wave number in free space. Using the parameters in Table 1 for the metaatom results in $\beta = 0$ at frequency $f_T$ (= 3 GHz, designated as the transition frequency).

As shown in Appendix Fig. 10, the radiation from the straight metaline (whose length is 120 mm = 12 × $p$) is right-hand circularly polarized (CP) and the direction of the maximum radiation is frequency-dependent: the direction is backward at frequencies below $f_T$, broadside at $f_T$, and

**TABLE 2.** Comparison with previous CP beam-steering antennas, where $\lambda_0$ is the working wavelength.

| | Frequency band | Antenna volume | Antenna thickness | Antenna footprint | Gain | Number of feed points | Scanning plane | Capability of continuous beam-steering |
|---|---|---|---|---|---|---|---|---|
| Proposed | Dual | $0.008\lambda_0^3$ | $0.028\lambda_0$ | $0.30\lambda_0^2$ | 5.0 dBi / 5.1 dBi | 2 | Elevation | Yes |
| [20] | Dual | $0.013\lambda_0^3$ | $0.014\lambda_0$ | $0.96\lambda_0^2$ | 7.1 dBi / 7.1 dBi | 2 | Azimuth | Yes |
| [21] | Single | $0.106\lambda_0^3$ | $0.197\lambda_0$ | $0.54\lambda_0^2$ | 8.1 dBi | 4 | Azimuth | No |
| [22] | Single | $0.068\lambda_0^3$ | $0.026\lambda_0$ | $2.66\lambda_0^2$ | ≈ 4 dBi | 4 | Azimuth | No |
| [23] | Single | $0.011\lambda_0^3$ | $0.013\lambda_0$ | $0.84\lambda_0^2$ | ≈ 4 dBi | 2 | Azimuth | Yes |
| [24] | Single | $0.015\lambda_0^3$ | $0.068\lambda_0$ | $0.22\lambda_0^2$ | Not clear | 2 | Elevation and azimuth | Yes |
| [25] | Single | $0.015\lambda_0^3$ | $0.017\lambda_0$ | $0.87\lambda_0^2$ | ≈ 8 dBi | 4 | Elevation and azimuth | Yes |
| [26] | Single | $0.005\lambda_0^3$ | $0.013\lambda_0$ | $0.41\lambda_0^2$ | ≈ 5 dBi | 2 | Elevation | No |

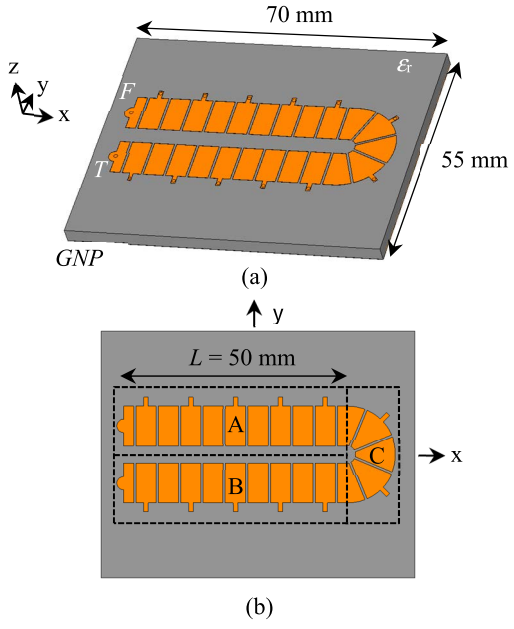


**FIGURE 4.** Bent P-type metaline, where sections *A* and *B* have a length of $L = 50$ mm. ($L = 0.24\lambda_g$ at $f_{LOW}$ and $L = 0.36\lambda_g$ at $f_{HIGH}$, with $\lambda_g$ being the guided wavelength). (a) Perspective view. (b) Top view.

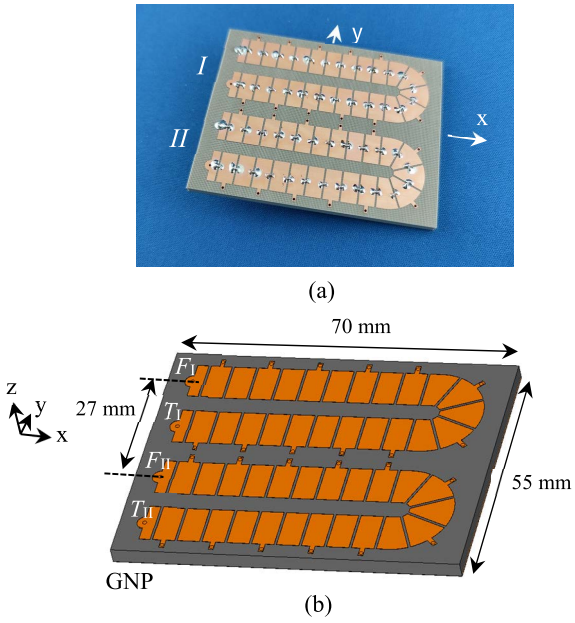


**FIGURE 5.** Array of the two bent P-type metalines. (a) Photo. (b) Parameter description.

forward at frequencies above $f_T$. Note that the number of the chips used for this metaline antenna is only 25 and hence the chip attachment by soldering is not a difficult problem. Also note that these chips might be replaced by interdigital capacitors [36], [37].

### B. BENT P-TYPE METALINE

A broadside beam is obtained only across a small frequency region centered at transition frequency $f_T = 3.0$ GHz, as shown in Appendix Fig. 10(b). In this subsection, we transform the tilted beam outside $f_T$ into a broadside beam at two frequencies: 2.65 GHz $\equiv f_{LOW}$ and 3.65 GHz $\equiv f_{HIGH}$.

For the transformation into a broadside pattern, we bend the straight metaline at its middle point, *M*, as shown in Fig. 4. The bent metaline is composed of three sections: straight sections *A* and *B*, and curved section *C*, which connects sections *A* and *B*. The grounded dielectric substrate supporting the bent metaline has a size of 70 mm × 55 mm × 3.2 mm, which corresponds to $0.618\lambda_{LOW} \times 0.486\lambda_{LOW} \times 0.028\lambda_{LOW}$ at $f_{LOW}$ and $0.852\lambda_{HIGH} \times 0.669\lambda_{HIGH} \times 0.039\lambda_{HIGH}$ at $f_{HIGH}$, where $\lambda_{LOW}$ and $\lambda_{HIGH}$ are the free-space wavelengths at $f_{LOW}$ and $f_{HIGH}$, respectively. This size leads to antenna features (2) through (4) described in the Introduction.

At low design frequency $f_{LOW}$ below $f_T$, the backward radiation (BRad) from section *A* in Fig. 4(b) is directed toward the negative x-space; conversely, the BRad from section *B* in

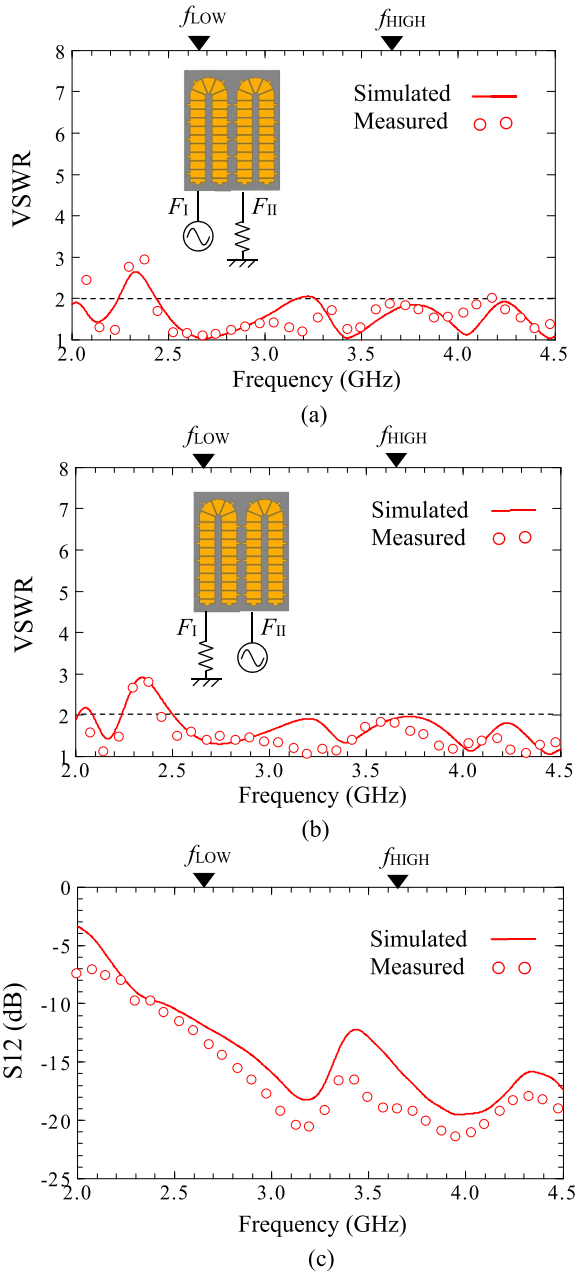


**FIGURE 6.** The input characteristics for the two bent metaline array, where the distance between the two bent metaline antennas is $d_{I-II}$ = 27 mm. (a) VSWR at $F_I$. (b) VSWR at $F_{II}$. (c) S12.

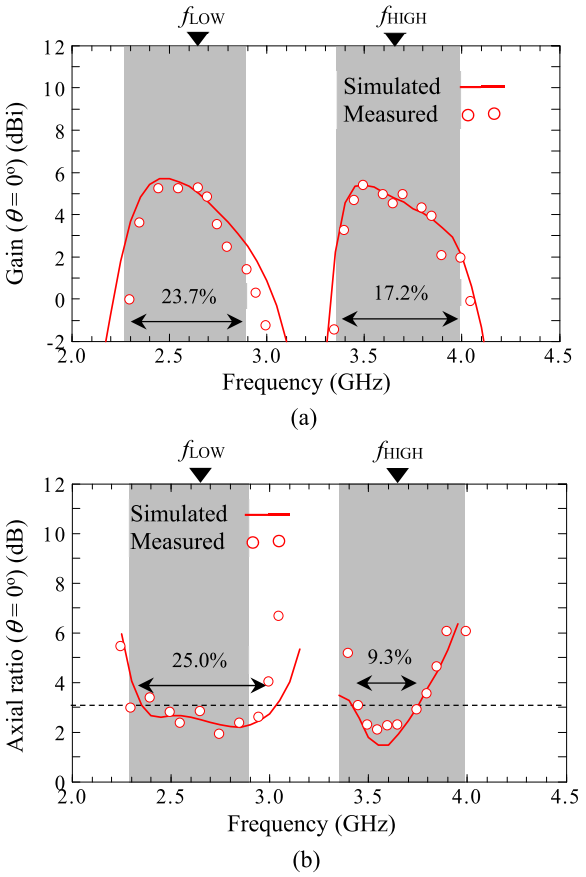


**FIGURE 7.** Frequency response for the gain and the axial ratio of the two bent metaline array excited in equal-amplitude/in-phase mode, where the distance between the two bent metaline antennas is $d_{I-II}$ = 27 mm. (a) Gain. (b) Axial ratio.

Fig. 4(b) is directed toward the positive x-space, as understood from Appendix Fig. 10(a). It follows that the superimposition of these two radiation waves forms a broadside beam, as shown in Appendix Fig. 11(a), which is described in detail in the recent work [28]. This type of broadside beam is also formed at high design frequency $f_{HIGH}$ above $f_T$, as shown in Appendix Fig. 11(b), where the forward radiation (FRad) from section *A* in Fig. 4(b), which is directed toward the positive x-space, is superimposed onto FRad from section *B*, which is directed toward the negative x-space, as understood from Appendix Fig. 10(c).

## III. NOVEL TWO-METALINE ARRAY ANTENNA

We fabricate a two-element array antenna to prepare beam-steering in section IV, as shown in Fig. 5. This is feature (5) described in Introduction. Both of the metalines are the same as the element presented in Section II. The size of the grounded dielectric substrate is also the same as that used in Section II: 55 mm × 70 mm × 3.2 mm (= $0.618\lambda_{LOW}$ × $0.486\lambda_{LOW}$ × $0.028\lambda_{LOW}$) so that features (2) to (4) are maintained. Points $F_I$ and $F_{II}$ in this figure are feed points, and $T_I$ and $T_{II}$ are terminal points, each of which is connected through a resistive load of $R_B$ (= 50 ohms) to the ground plane. The distance between the two bent metalines in the y-direction is $d_{I-II}$ = 27 mm, which is $0.239\lambda_{LOW}$ at $f_{LOW}$ and $0.329\lambda_{HIGH}$ at $f_{HIGH}$.

Fig. 6 shows the frequency response of the input characteristics at feed points $F_I$ and $F_{II}$. At frequencies around design frequencies $f_{LOW}$ and $f_{HIGH}$, the VSWR at $F_I$ and at $F_{II}$ is small, with a value of less than two, as desired. The mutual coupling between $F_I$ and $F_{II}$, *i.e.*, S12, is also acceptably

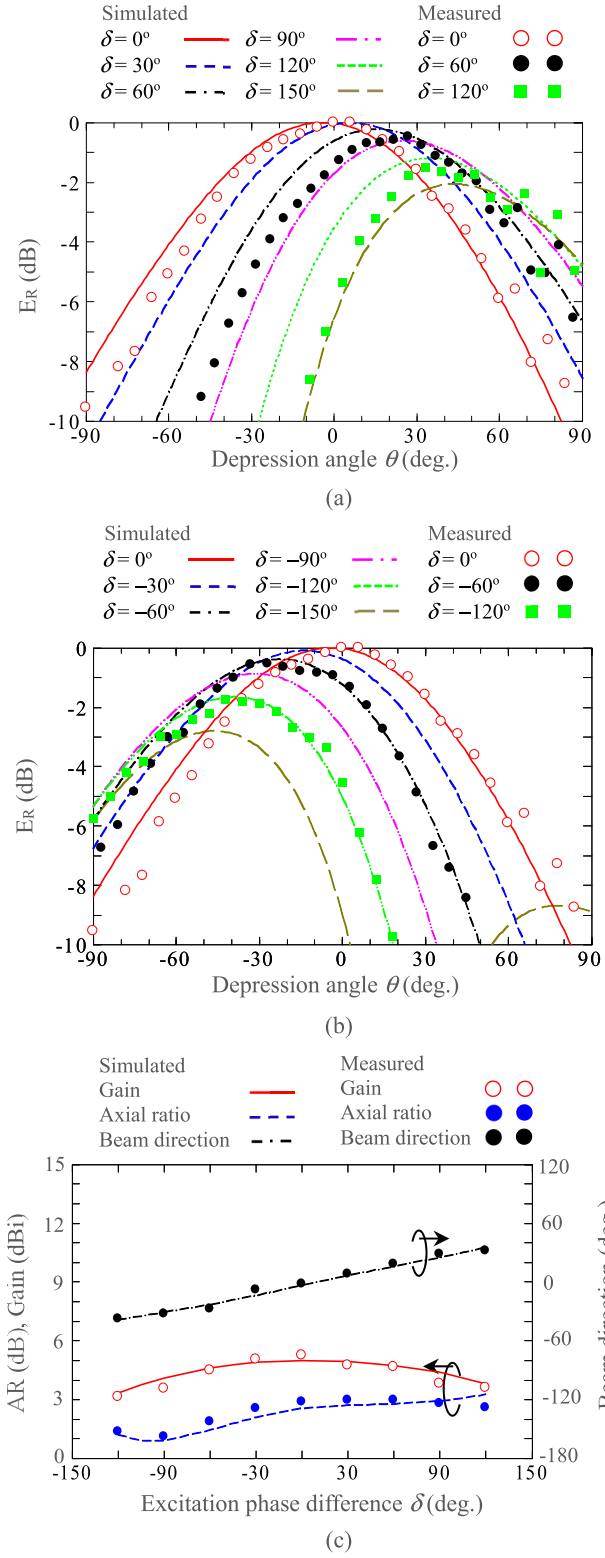


**FIGURE 8.** Beam-steering at $f_{LOW} = 2.65$ GHz with relative excitation phase $\delta$ as a parameter. (a) For positive $\delta$. (b) For negative $\delta$. The radiation patterns in (a) and (b) are all normalized to the maximum field intensity for $\delta = 0°$. Cross-polarization component $E_L$ is less than $-10$ dB and does not appear at this scale. (c) Beam direction across a range of $\delta = -120°$ to $\delta = +120°$, together with the gain and axial ratio in the beam direction.

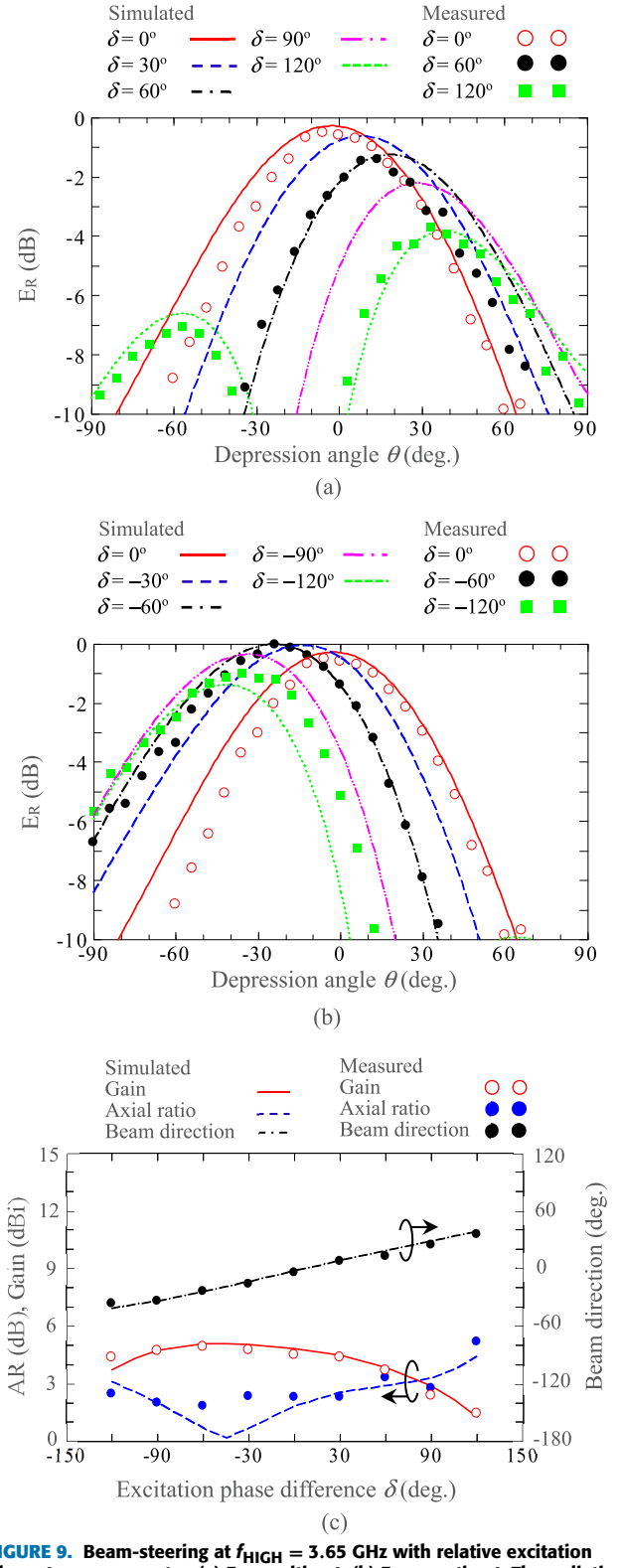


**FIGURE 9.** Beam-steering at $f_{HIGH} = 3.65$ GHz with relative excitation phase $\delta$ as a parameter. (a) For positive $\delta$. (b) For negative $\delta$. The radiation patterns in (a) and (b) are all normalized to the maximum field intensity for $\delta = -60°$. Cross-polarization component $E_L$ is less than $-10$ dB and does not appear at this scale. (c) Beam direction across a range of $\delta = -120°$ to $\delta = +120°$, together with the gain and axial ratio in the beam direction.

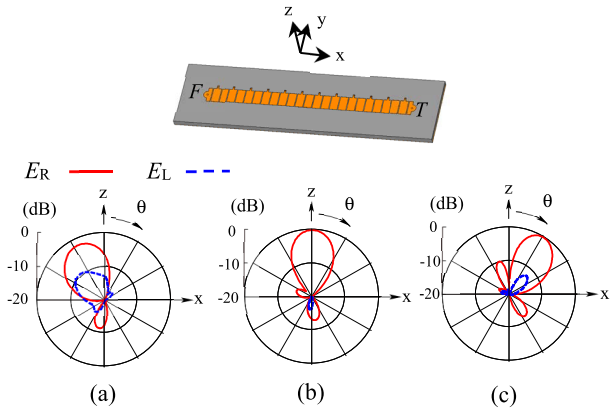


**FIGURE 10.** Radiation from the straight P-type metaline when frequency $f$ is changed. The straight P-type metaline has a length of 120 mm. (a) Backward beam at $f = 2.65$ GHz. (b) Broadside beam at $f_T = 3.0$ GHz. (c) Forward beam at $f = 3.65$ GHz.

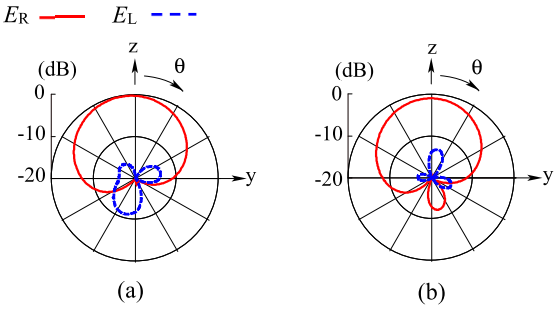


**FIGURE 11.** Simulated radiation pattern of the single bent P-type metaline (Fig. 4), where length 120 mm = $0.57\lambda_g$ at $f_{LOW}$ and $0.86\lambda_g$ at $f_{HIGH}$. The patterns are normalized to the maximum radiation intensity at $f_{LOW}$. (a) At $f_{LOW} = 2.65$ GHz. (b) At $f_{HIGH} = 3.65$ GHz.

small. These simulation results are in reasonable agreement with the measured results.

The frequency responses of the gain and the axial ratio (AR) in the z-direction are shown in Fig. 7, where the feed points are excited in equal-amplitude/in-phase mode. The maximum gain is 5.0 dBi at $f_{LOW}$ and 5.1 dBi at $f_{HIGH}$, which are larger compared with those for the single bent metaline by 1.6 dB at $f_{LOW}$ and 2.4 dB at $f_{HIGH}$. The gain bandwidth for a $-3$ dB gain drop criterion is 23.7% around $f_{LOW}$ and 17.2% around $f_{HIGH}$, while the CP bandwidth for a 3-dB axial ratio criterion is 25.0% around $f_{LOW}$ and 9.3% around $f_{HIGH}$. It follows from Figs. 6 and 7 that the array has a bandwidth that is reasonable for practical applications. Note that the radiation pattern in equal-amplitude/in-phase mode is included in Figs. 8(a) and (b) and Figs. 9(a) and (b) of the next section. See lines of $\delta = 0°$.

## IV. BEAM-STEERING

To steer the CP beam in the H-plane (y-z plane), we excite feed points $F_I$ and $F_{II}$ in equal-amplitude/different-phase mode, where the phase at feed point $F_{II}$ differs from that at $F_I$ by $\delta$ ($\equiv \angle F_{II} - \angle F_I$).

Fig. 8(a) shows the radiation pattern in the H-plane with $\delta$ as a parameter, where design frequency $f_{LOW}$ is used. The beam is directed toward the positive y-space (positive $\theta$ direction) when $\delta > 0$, *i.e.* the excitation phase at $F_I$ lags the phase at $F_{II}$. Conversely, the radiation beam in Fig. 8(b) at $f_{LOW}$ is directed toward the negative y-space (negative $\theta$ direction) when $\delta < 0$, *i.e.* the excitation phase at $F_I$ leads the phase at $F_{II}$. The beam direction at $f_{LOW}$ is summarized in Fig. 8(c), where the gain and axial ratio (AR) in the beam direction are also presented. It is found that the beam direction varies almost linearly. The variation from the maximum gain at $f_{LOW}$ (5.0 dBi) is small: approximately 1.7 dB. The simulated results are validated by the measured results, which are in reasonably good agreement.

Similar behavior of the steered beam at high design frequency $f_{HIGH}$ is found and shown in Figs. 9(a) and (b). An almost linear change in the beam direction is seen in Fig. 9(c). The gain and axial ratio in the beam direction are also illustrated in this figure. The variation from the maximum gain at $f_{HIGH}$ (5.1 dBi) is small, as is seen at $f_{LOW}$: approximately 1.4 dB for AR $\leq$ 3 dB. The measured results validate the simulated results in this case, as well.

## V. CONCLUSION

A circularly polarized (CP), beam-steerable, small antenna with dual-band operation has been realized, where two bent P-type metalines are arrayed within a small volume that corresponds to 0.62 wavelength × 0.49 wavelength × 0.028 wavelength at low design frequency $f_{LOW}$ (volume $= 0.008\lambda^3_{LOW}$). The realization is performed using four steps.

Firstly, characteristics of a straight metaline composed of P-type metaatoms are summarized. It is clarified that a CP broadside beam appears only around transition frequency $f_T$. Secondly, the straight CP metaline is bent to form three sections: straight sections A and B (both having the same length) and a small curved section, C, which connects sections A and B. It is revealed that a CP broadside beam is generated at two frequencies outside $f_T$: low design frequency $f_{LOW} < f_T$ and high design frequency $f_{HIGH} > f_T$.

Thirdly, two bent metaline elements, I and II, are arrayed within a small area that corresponds to 0.62 wavelength × 0.49 wavelength at $f_{LOW}$. The antenna characteristics for the two-element array excited in equal-amplitude/in-phase mode are investigated. It is found that the array forms a CP broadside beam at frequencies $f_{LOW}$ and $f_{HIGH}$, with a gain increase (compared to the gain for the single bent metaline) of 1.6 dB at $f_{LOW}$ and 2.4 dB at $f_{HIGH}$.

Fourthly, beam-steering in the H-plane is performed by changing the excitation phase difference between the two feed points, $\delta$. The beam direction changes almost linearly within a region of $-120° \leq \delta \leq 120°$. The beam with an axial ratio of less than 3 dB is steered from $-40°$ to $+30°$ at $f_{LOW}$ and from $-40°$ to $+25°$ at $f_{HIGH}$. During the beam steering, the gain deviation at $f_{LOW}$ from its maximum value

is small: 1.7 dB for a 3 dB axial ratio criterion. A similar small gain deviation of 1.4 dB is observed at $f_{\mathrm{HIGH}}$.

Finally, the following comment is made here. The design frequencies of the proposed antenna can be moved to different frequencies using a scaling technique for configuration parameters.

## APPENDIX

Comparison with previous CP beam-steering antennas is shown in Table 2. Simulation results for the radiation field of a metaline antenna and a bend metaline antenna are shown in Fig. 10 and Fig. 11, respectively [28].

## ACKNOWLEDGMENT

The authors thank Victor Shkawrytko for his assistance in the preparation of this manuscript.

## REFERENCES

[1] J. Kraus and R. Marhefka, *Antennas*, 3rd ed. New York, NY, USA: McGraw-Hill, 2002.
[2] Y. Tawk, "A dynamic dual tapered 3-D printed nested helical antenna," *IEEE Trans. Antennas Propag.*, vol. 68, no. 2, pp. 697–702, Feb. 2020.
[3] Y. Letestu and A. Sharaiha, "Broadband folded printed quadrifilar helical antenna," *IEEE Trans. Antennas Propag.*, vol. 54, no. 5, pp. 1600–1604, May 2006.
[4] J. Kaiser, "The Archimedean two-wire spiral antenna," *IRE Trans. Antennas Propag.*, vol. 8, no. 3, pp. 312–323, May 1960.
[5] J. J. H. Wang, "The spiral as a traveling wave structure for broadband antenna applications," *Electromagnetics*, vol. 20, no. 4, pp. 323–342, Jul. 2000.
[6] H. Nakano, K. Nogami, S. Arai, H. Mimaki, and J. Yamauchi, "A spiral antenna backed by a conducting plane reflector," *IEEE Trans. Antennas Propag.*, vol. AP-34, no. 6, pp. 791–796, Jun. 1986.
[7] H. Nakano, S. Okuzawa, K. Ohishi, H. Mimaki, and J. Yamauchi, "A curl antenna," *IEEE Trans. Antennas Propag.*, vol. 41, no. 11, pp. 1570–1575, Nov. 1993.
[8] S. M. O'Kane and V. F. Fusco, "Circularly polarized curl antenna lens with manual tilt properties," *IEEE Trans. Antennas Propag.*, vol. 57, no. 12, pp. 3984–3987, Dec. 2009.
[9] J. Wu, S. K. Khamas, and G. G. Cook, "Moment method analysis of a conformal curl antenna printed within layered dielectric cylindrical media," *IEEE Trans. Antennas Propag.*, vol. 61, no. 7, pp. 3912–3917, Jul. 2013.
[10] K. Hirose, T. Shibasaki, and H. Nakano, "Fundamental study on novel loop-line antennas radiating a circularly polarized wave," *IEEE Antennas Wireless Propag. Lett.*, vol. 11, pp. 476–479, 2012.
[11] Q. Yang, X. Zhang, N. Wang, X. Bai, J. Li, and X. Zhao, "Cavity-backed circularly polarized self-phased four-loop antenna for gain enhancement," *IEEE Trans. Antennas Propag.*, vol. 59, no. 2, pp. 685–688, Feb. 2011.
[12] H. Nakano, H. Takeda, T. Honma, H. Mimaki, and J. Yamauchi, "Extremely low-profile helix radiating a circularly polarized wave," *IEEE Trans. Antennas Propag.*, vol. 39, no. 6, pp. 754–757, Jun. 1991.
[13] H. Nakano, H. Takeda, Y. Kitamura, H. Mimaki, and J. Yamauchi, "Low-profile helical array antenna fed from a radial waveguide," *IEEE Trans. Antennas Propag.*, vol. 40, no. 3, pp. 279–284, Mar. 1992.
[14] H. Nakano, Y. Shinma, and J. Yamauchi, "A monofilar spiral antenna and its array above a ground plane-formation of a circularly polarized tilted fan beam," *IEEE Trans. Antennas Propag.*, vol. 45, no. 10, pp. 1506–1511, Oct. 1997.
[15] A. Kuramoto, T. Yamane, R. Shimizu, and N. Endo, "Compact mobile antenna system with a new developed simple auto tracking method for satellite communications," *IEICE Trans. B*, vol. J71-B, no. 11, pp. 1389–1392, Nov. 1988.
[16] W. L. Stutzman and G. A. Thiele, *Antenna Theory and Design*, 2nd ed. New York, NY, USA: Wiley, 1998.
[17] Z. N. Chen, D. Liu, H. Nakano, X. Qing, and T. Zwick, Eds., *Handbook of antenna Technologies*. Singapore: Springer, 2016.
[18] K. Hirose, S. Okazaki, and H. Nakano, "Double loop antennas for a circularly polarized tilted beam," *IEICE Trans. B*, vol. J85-B, no. 11, pp. 1934–1943, Nov. 2002.
[19] H. Nakano, "A numerical approach to line antennas printed on dielectric materials," *Comput. Phys. Commun.*, vol. 68, nos. 1–3, pp. 441–450, Nov. 1991.
[20] H. Nakano, T. Abe, and J. Yamauchi, "Compound metaloop antenna for circularly polarized beam steering," *IEEE Access*, vol. 9, pp. 79806–79815, 2021.
[21] H. Zhou, A. Pal, A. Mehta, D. Mirshekar-Syahkal, and H. Nakano, "A four-arm circularly polarized high-gain high-tilt beam curl antenna for beam steering applications," *IEEE Antennas Wireless Propag. Lett.*, vol. 17, pp. 1034–1038, 2018.
[22] H. Nakano, T. Abe, and J. Yamauchi, "Planar reconfigurable antennas using circularly polarized metalines," *IEEE Antennas Wireless Propag. Lett.*, vol. 18, no. 5, pp. 1006–1010, May 2019.
[23] H. Nakano, T. Abe, T. Kawano, A. Mehta, and J. Yamauchi, "Azimuth angle estimation for a reduced radiation region formed by a metaspiral antenna," *IEEE Access*, vol. 7, pp. 78289–78297, 2019.
[24] C. Deng, Y. Li, Z. Zhang, and Z. Feng, "A hemispherical 3-D null steering antenna for circular polarization," *IEEE Antennas Wireless Propag. Lett.*, vol. 14, pp. 803–806, 2015.
[25] N. R. Labadie, S. K. Sharma, and G. M. Rebeiz, "A circularly polarized multiple radiating mode microstrip antenna for satellite receive applications," *IEEE Trans. Antennas Propag.*, vol. 62, no. 7, pp. 3490–3500, Jul. 2014.
[26] S. Maddio, "A circularly polarized switched beam antenna with pattern diversity for WiFi applications," *IEEE Antennas Wireless Propag. Lett.*, vol. 16, pp. 125–128, 2017.
[27] *Computer Simulation Technology GmbH*. Microwave Studio. Darmstadt, Germany. Accessed: May 2022. [Online]. Available: http://www.cst.com
[28] T. Abe, J. Yamauchi, and H. Nakano, "A U-Shaped low-profile metaline array antenna for a circularly polarized fan-beam across two frequency bands," *IEEE Antennas Wireless Propag. Lett.*, vol. 21, no. 6, pp. 1268–1272, Jun. 2022.
[29] A. Mehta, D. Mirshekar-Syahkal, and H. Nakano, "Beam adaptive single arm rectangular spiral antenna with switches," *IEE Proc. Microwaves, Antennas Propag.*, vol. 153, no. 1, pp. 13–18, Feb. 2006.
[30] C. G. Christodoulou, Y. Tawk, S. A. Lane, and S. R. Erwin, "Reconfigurable antennas for wireless and space applications," *Proc. IEEE*, vol. 100, no. 7, pp. 2250–2261, Jul. 2012.
[31] H. Nakano, Y. Kameta, T. Kawano, A. Mehta, A. Pal, A. Skippins, and J. Yamauchi, "Antenna system composed of T-shaped elements coupled to an open radial waveguide," *IEEE Trans. Antennas Propag.*, vol. 66, no. 2, pp. 550–563, Feb. 2018.
[32] R. Mailloux, *Phased Array Antenna Handbook*, 2nd ed. Norwood, MA, USA: Artech House, 2005.
[33] C. A. Balanis, Ed., *Modern Antenna Handbook*. Hoboken, NJ, USA: Wiley, 2008.
[34] C. Caloz and T. Itoh, *Electromagnetic Metamaterials*. Hoboken, NJ, USA: Wiley, 2006.
[35] H. Nakano, K. Sakata, and J. Yamauchi, "Linearly and circularly polarized radiation from metalines," in *Proc. iWAT*, Cocoa Beach, FL, USA, Mar. 2016, pp. 142–143.
[36] G. D. Alley, "Interdigital capacitors and their application to lumped-element microwave integrated circuits," *IEEE Trans. Microw. Theory Techn.*, vol. MTT-18, no. 12, pp. 1028–1033, Dec. 1970.
[37] L. Zhu and K. Wu, "Accurate circuit model of interdigital capacitor and its application to design of new quasi-lumped miniaturized filters with suppression of harmonic resonance," *IEEE Trans. Microw. Theory Techn.*, vol. 48, no. 3, pp. 347–356, Mar. 2000.

**HISAMATSU NAKANO** (Life Fellow, IEEE) held positions as a Visiting Associate Professor with Syracuse University, from March 1981 to September 1981; and a Visiting Professor with the University of Manitoba, from March 1986 to September 1986, the University of California at Los Angeles, Los Angeles, from September 1986 to March 1987, and Swansea University, U.K., from July 2016 to September 2019. He has been with Hosei University, since 1973, where he is currently a Professor Emeritus and a special-appointment Researcher with the Electromagnetic Wave Engineering Research Institute attached to the graduate school. He has published over 360 articles in peer-reviewed journals and 11 books/book chapters, including *Low-Profile Natural and Metamaterial Antennas* (IEEE Press–Wiley, 2016). His significant contributions are the development of five integral equations for line antennas in free space and printed on a dielectric substrate; the invention of an L-shaped wire/strip antenna feeding method; and the realization of numerous wideband antennas, including curl, metaspiral, metahelical, and body of revolution antennas. His other accomplishments include design of antennas for GPS, personal handy phones, space radio, electronic toll collection, RFID, UWB, and radar. He has been awarded 78 patents, including "A Curl Antenna Element and Its Array" (Japan). His research interests include numerical methods for low- and high-frequency antennas and optical waveguides. He served as a member for the IEEE APS Administrative Committee, from 2000 to 2002; and a Region 10 Representative, from 2001 to 2010. He received the H. A. Wheeler Award, in 1994; the Chen-To Tai Distinguished Educator Award, in 2006; and the Distinguished Achievement Award, in 2016, all from the IEEE Antennas and Propagation Society. He was also a recipient of The Prize for Science and Technology from Japan's Minister of Education, Culture, Sports, Science and Technology, in 2010. Most recently, he was selected as a recipient of the Antenna Award of the European Association on Antennas and Propagation (EurAAP), in 2020. He is an Associate Editor of several scientific journals and magazines, including *Electromagnetics*.

**TOMOKI ABE** (Member, IEEE) was born in Miyagi, Japan, in August 1994. He received the B.E., M.E., and Ph.D. degrees in electronics and electrical engineering from Hosei University, Tokyo, Japan, in 2017, 2019, and 2022, respectively. He is a member of the Institute of Electronics, Information and Communication Engineers of Japan.

**JUNJI YAMAUCHI** (Life Fellow, IEEE) was born in Nagoya, Japan, in August 1953. He received the B.E., M.E., and Dr.E. degrees from Hosei University, Tokyo, Japan, in 1976, 1978, and 1982, respectively. From 1984 to 1988, he served as a Lecturer with the Electrical Engineering Department, Tokyo Metropolitan Technical College. Since 1988, he has been a member of the Faculty of Hosei University, where he is currently a Professor with the Electrical and Electronic Engineering Department. He is the author of *Propagating Beam Analysis of Optical Waveguides* (Research Studies Press, 2003). His research interests include optical waveguides, polarization converters, and circularly polarized antennas. He is a member of the Optical Society of America and the Institute of Electronics, Information and Communication Engineers of Japan.